Proceedings of the Twenty-seventh (2017) International Ocean and Polar Engineering Conference **www.isope.org**
San Francisco, CA, USA, June 25-30, 2017

ISBN 978-1-880653-97-5; ISSN 1098-6189

Numerical Investigations of Open-water Performance of Contra-Rotating Propellers

Dongya He[1], *Decheng Wan*[1*], *Xinguo Yu*[2]
[1] Collaborative Innovation Center for Advanced Ship and Deep-Sea Exploration, State Key Laboratory of Ocean Engineering, School of Naval Architecture, Ocean and Civil Engineering, Shanghai Jiao Tong University, Shanghai, China
[2] China Ship Development and Design Center, Shanghai Branch, China
[*] Corresponding author

ABSTRACT

In this paper, the open-water performance of contra-rotating propellers (CRPs) has been investigated using CFD method with sliding mesh model dealing with the relative rotation of CRPs. Results show that CRPs exhibits apparent periodical unsteady thrust and torque. After FFT (Fast Fourier Transform) of those forces coefficients, results show that they are composed of amplitudes of 8 times, 16 times and 24 times shaft frequency. Time-averages of predicted unsteady thrust and torque agree well with their experimental counterparts. On the other hand, CRPs' wake flow field has been analyzed in detail to prove that CRPs is superior in efficiency and stability to single propeller since majority of rotational energy produced by front propeller can be almost fully recovered.

KEY WORDS: CRPs; open-water performance; energy saving device; CFD; sliding mesh method.

INTRODUCTION

Right now, the majority of ships operating in the world are powered by diesel engine, with traditional shaft propeller as their main propulsion type. This type is poor in efficiency, vibration quality and easy to cause propeller cavitation. Every year, carbon emission in ship operation accounts a big proportion than other industries. On the other hand, in order to reduce costs in operation, carriers such as container ship become bigger and faster, thus propeller needs bigger diameter and become more and more heavier. On the other hand, such conventional single screw propulsion mode has technically reached its limits due to engine power, propeller loading and weight, hull vibration, maneuverability, etc.(Kim et al., 2002), therefore it's essential to seek for more advanced propelling system.

In this circumstance, IMO put forward three indexes, namely EEDI (Energy Efficiency Design Index), EEOI (Energy Efficiency Operational Index), SEEMP (Ship Energy Efficiency Management Plan) to promote "green" ship' development. A lot of operating ships in China are going to be banned for mismatching those standards. Therefore, researchers have designed many types of energy-saving devices to improve propeller' propulsion efficiency. There are three main reasons that will degrade propulsion efficiency which are non-uniform inflow at propeller disk, vortex resistance at hub and blade tip and rotational wake flow behind propeller. Wake equalizing duct, propeller boss cap fin and CRPs are the common energy saving devicts. they can improve efficiency from 2% to 8%. CRPs has two conventional propellers which rotate coaxially in reverse direction. The rear propeller can greatly recover vortex kinetic energy left by front propeller, furthermore, CRPs can weaken unbalanced moment, thus it has been extensively applied to propel torpedo which needs high standard of course keeping stability.

Since 1970's, many researchers in the world have investigated steady and unsteady open-water performance of CRPs. Some of them in David W Taylor Naval Ship R&D Center (1976) tested two sets of CRPs, their model and experimental data have been used by many CFD researchers. Yang (1992) developed the steady and unsteady lifting surface models which are based on potential flow theory. Since the late 1990's, CFD method has been increasingly used in marine hydrodynamics owing to the rapid improvement in computer capabilities and numerical method. Because CFD method is based on actual fluid control functions (Navier-Stokes equations) which take the viscosity and rotation into account, thus it can correctly model nonlinear wake deformation and flow separation due to heavy loading. Up to now, MRF (Multiple Reference Frame) method, overset mesh method, and sliding mesh method are the three main techniques dealing with propeller' rotation. MRF method can only be used to predict steady forces, in other words, dynamic flow field cannot be obtained. Though this method has high efficiency, its precision is not so good as overset mesh method and sliding mesh method. Overset mesh method has been extensively applied to handle problems that have multiple moving objects with many degrees of freedom. Different grids will exchange their information through an interpolating code named SUGGAR++ (Noack et al., 2009) on the overlapping area of sliding mesh. At sacrifice of relatively large of computing resources, this method will guarantee high accuracy. Shen, et al (2012) carried out KCS self-propulsion and maneuvering by CFD solver naoe-FOAM-SJTU with overset mesh technique, predicted results agree well with their experimental data. Comparing with MRF and overset mesh method, sliding mesh method keeps equal precision as overset mesh method, but its computing efficiency is greatly improved since this method only needs interpolation between overlapping area of rotational region and static region. Wu (2016) compared accuracy and computing

efficiency of those three method applied to numerical prediction of open-water performance of single propeller. Based on sliding mesh method, Zhou (2014) investigated unsteady flow around wind turbines with different blades numbers. Wang, et at (2012) studied two sets of CRPs' open-water performance developed by David W Taylor Naval Ship R&D Center using CFD method, numerical predicted results agree well with their experimental counterparts, furthermore, he investigated CRPs' periodical unsteady thrust and torque in detail.

Considering accuracy and computing efficiency, sliding mesh method was adopted to settle CRPs' rotation in this paper. In order to make it easy to illustrate CRPs' superiority to single propeller, CRPs' front propeller called single propeller has also been simulated independently.

NUMERICAL METHOD

In this paper, single phase flow solver, pimpleDyMFoam, has been used, its capability of solving unsteady problem could help to simulate CRPs' unsteady flow field well. The Reynolds Averaged Navier-Stokes(RANS) functions with turbulence model $k-\omega\ SST$ which was put forward by Menter (2003) have been verified by many scholars to be efficient to simulate propeller' flow field. A second-order TVD limited linear scheme was used to discretize the convection terms in RANS functions while the diffusion terms were discretized by a second-order central difference scheme. Pimple algorithm was used to solve coupling problem of pressure and velocity. Time step was equal to 1.157e-04 second so the propeller could rotate about 1 degree.

Governing Equations

For the incompressible viscous fluid flow, the continuity equation and RANS equations are expressed as follows:

$$\frac{\partial u_i}{\partial x_i}=0 \tag{1}$$

$$\frac{\partial}{\partial t}(u_i)+\frac{\partial}{\partial x_j}(u_i u_j)=-\frac{\partial p}{\partial x_j}+\frac{1}{\mathrm{Re}}\frac{\partial}{\partial x_j}(\frac{\partial u_i}{\partial x_j}+\frac{\partial u_j}{\partial x_i})+\frac{\partial}{\partial x_j}(-\overline{u_i' u_j'}) \tag{2}$$

Where u_i are averages of velocity components in three directions; j (=1, 2, 3) means different direction; R_e is Reynolds number; $-\overline{u_i' u_j'}$ are Reynolds stress.

Sliding Mesh Method

Supposing that the open-water calculation of single propeller is going to be simulated, the computation domain will be divided into two parts. One of them surrounds and rotates with propeller, the other is the residual domain and keeps static. Both domains will exchange information in the overlapping meshes. Grid numbers on both surfaces are not strictly required to be consistent, but flux must be equal, or numerical computing process will become diverging.

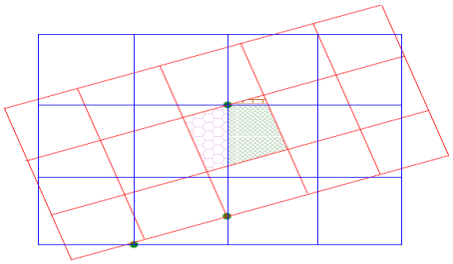

Fig. 1 Diagram of sliding mesh

Fig. 1 shows diagram of the overlapping area of sliding meshes. In order to keep flux transmitting and flow field information exchanging reasonable, interpolation manner is based on weight coefficient meaning how much contribution one cell on one side of sliding surfaces makes to the other side. For example, blue mesh and red mesh are assumed to be the main surface and slave surface respectively. The weight one cell owes from main surface to the cell in slave surface in the overlapping cell is the ratio how much overlapping area the cell in main surface accounts.

COMPUTATIONAL OVERVIEWS

Geometric Model and Case

One of test models of CRPs developed by David W Taylor Naval Ship R&D Center has been chosen as the object of study. The front propeller is named DTMB3686 and the rear named DTMB3687.

Table 1. Parameters of CRPs

Parameters	DTMB3686	DTMB3687
Diameter/mm	305.2	299.1
Blade number	4	4
$(P/D)_{0.7r}$	1.291	1.326
Area ratio	0.303	0.324
Rotating direction	Left	Wright
Section	NACA66mod/a=0.8	NACA66mod/a=0.8

Modeling of CRPs is based on propeller projection theory(Wang, et al., 2007), as Fig. 2 shows. The two dimensional coordinates of blade sections can be transformed into global three dimensional coordinates by Eqs. 3~10.

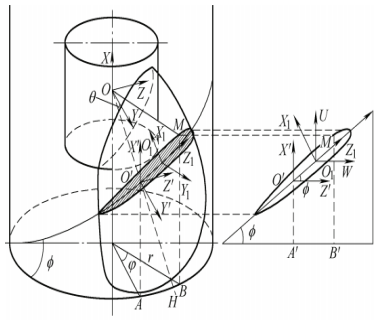

Fig. 2 Diagram of propeller project theory

$$x_{up}=C_{(r)}(s-0.5)\sin\varphi_{(r)}-(f_{(s)}+t_{(s)})\cos\varphi_{(r)}+x_{(r)} \tag{3}$$

$$\theta_{up(r)}=C_{(r)}(s-0.5)\frac{\cos\varphi_{(r)}}{r}+(f_{(s)}+t_{(s)})\frac{\sin\varphi_{(r)}}{r}+\theta_{(r)} \tag{4}$$

$$y_{up(r)}=r\cos\theta_{\mathrm{up(r)}} \tag{5}$$

$$z_{up(r)}=r\sin\theta_{up(r)} \tag{6}$$

$$x_{down(r)}=C_{(r)}(s-0.5)\sin\varphi_{(r)}-(f_{(s)}-t_{(s)})\cos\varphi_{(r)}+x_{(r)} \tag{7}$$

$$\theta_{down(r)}=C_{(r)}(s-0.5)\frac{\cos\varphi_{(r)}}{r}+(f_{(s)}-t_{(s)})\frac{\sin\varphi_{(r)}}{r}+\theta_{(r)} \tag{8}$$

$$y_{down(r)}=r\cos\theta_{down(r)} \tag{9}$$

$$z_{down(r)}=r\sin\theta_{down(r)} \tag{10}$$

Where $x_{(r)}$ is rake downward, $\theta_{(r)}$ is heeling angle, $\varphi_{(r)}$ is angle of pitch, $C_{(r)}$ chord length, s is dimensionless location of hydrofoil points along chord, $f_{(s)}$ is camber, $t_{(s)}$ is maximum thickness of hydrofoil. After lofting of different blade sections, the final CRPs model was built as what Fig. 3 shows. In order to analyze CRPs' superiority, single propeller, DTMB3686, has also been calculated, as Fig. 4 shows. There are five cases in this paper. Thrust and torque of CRPs were computed when inlet coefficient, J, is at 0.7, 0.8, 0.9, 1.0, 1.1. Front and rear propeller rotated at the revolution rate of 12 in reverse direction.

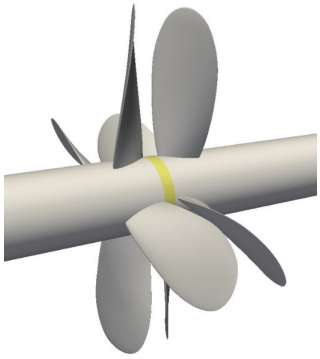

Fig. 3 CRPs model

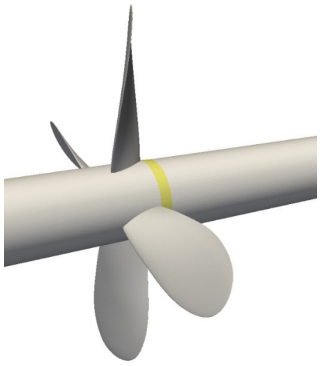

Fig. 4 Single propeller model

Computational Domain and Boundary Conditions

As Fig. 5 shows, the larger domain extends from -3.5D to 5D in x direction with diameter of 3 times front propeller'. There are two sets of sliding surfaces surrounding front and rear propellers respectively.

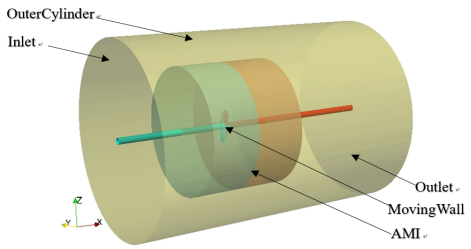

Fig. 5 Global computational domain

At the inlet, U is inflow velocity while pressure gradient is zero. At the outlet, pressure is zero while velocity gradient is zero. Boundary condition of "outerCylinder" is symmetry. Non-slipping wall condition is applied to propeller and stem surfaces.

Mesh Configuration

Fig. 6 shows global mesh created by software , ICEM, who is adept at creation of O-block mesh. There are about 4.5 million cells in global mesh. As Fig. 7 shows, mesh has been refined around area of CRPs in order to capture crucial flow field information..

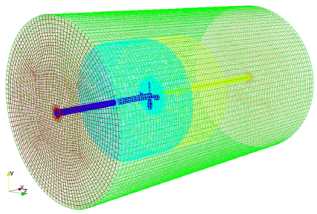

Fig. 6 Global mesh

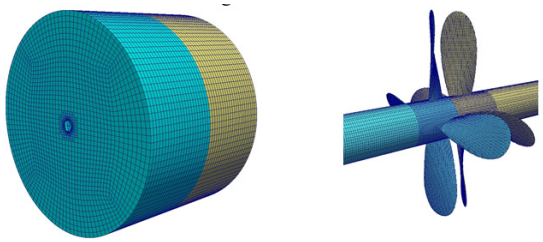

(a) Sliding surfaces mesh (b) Propeller grid

Fig. 7 Local mesh

NUMERICAL RESULTS AND ANALYSES

Numerical Results

First, some coefficients need to be defined that will help to analyze the open-water performance of CRPs. They are defined as follow:

$$J = \frac{V}{nD_F} \tag{11}$$

$$K_{TF} = \frac{T_F}{\rho n^2 D_F^4} \tag{12}$$

$$K_{QF} = \frac{Q_F}{\rho n^2 D_F^5} \tag{13}$$

$$K_{TA} = \frac{T_A}{\rho n^2 D_F^4} \tag{14}$$

$$K_{QA} = \frac{Q_A}{\rho n^2 D_F^5} \tag{15}$$

$$K_T = K_{TF} + K_{TA} \tag{16}$$

$$K_Q = K_{QF} + K_{QA} \tag{17}$$

$$\eta = \frac{JK_T}{2\pi K_Q} \tag{18}$$

Where subscript F means front propeller and subscript A means rear propeller. K_T and K_Q are hydrodynamic coefficients of CRPs.

Fig. 8 shows evident unsteady forces of CRPs when J is 1. As we can see, there are eight small periods after front or rear propeller rotates 360 degrees, that's because both propellers have four blades. What's more, the amplitudes of force coefficients' variation suffered by front propeller are larger than rear propeller while time-averages of unsteady forces are in reverse. After FFT of those forces coefficients, Fig. 9 shows that they are mainly composed of amplitudes of 8 times, 16 times, and 24 times shaft frequency with their amplitudes decreasing as

exponential function, this phenomenon illustrates strong interaction between front and rear propellers . Fig. 10~12 reflect open-water performance of front propeller, rear propeller and CRPs respectively. Numerical results agree well with their experimental counterparts. Fig. 10 shows errors of K_T are around 5% while errors of K_Q are around 1%. Fig. 11 tells that predicted K_T is lower than experimental data about 1.893% while predicted K_Q is relatively larger than experimental data about 8%. That's because the rear propeller works in the complex wake flow of front propeller. More accurate simulation may require more refined mesh and advanced turbulence model. Fig. 12 shows averages of forces coefficient of CRPs. Errors of K_T and K_Q are around 2% and 4.5% respectively.

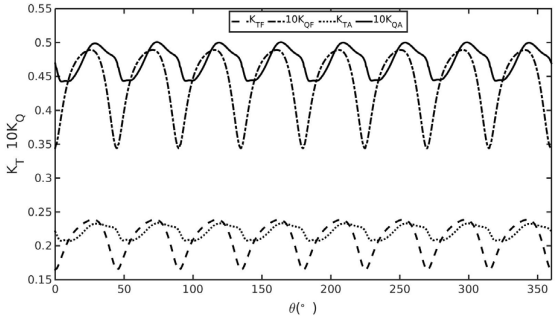

Fig. 8 Time history of hydrodynamic coefficients of CRPs

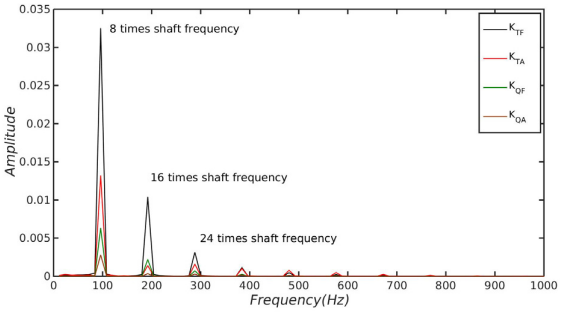

Fig. 9 Fast fourier transform of thrust and torque coefficients

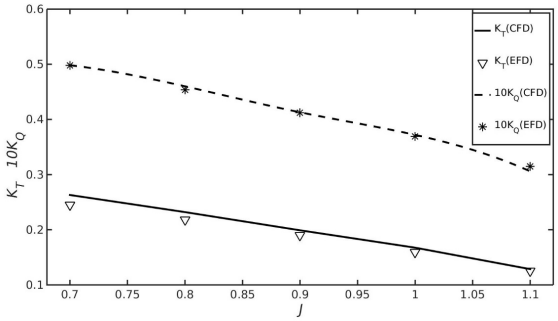

Fig. 10 Open-water performance curves of front propeller

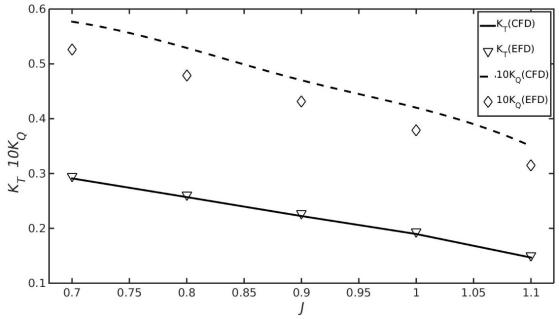

Fig. 11 Open-water performance curves of rear propeller

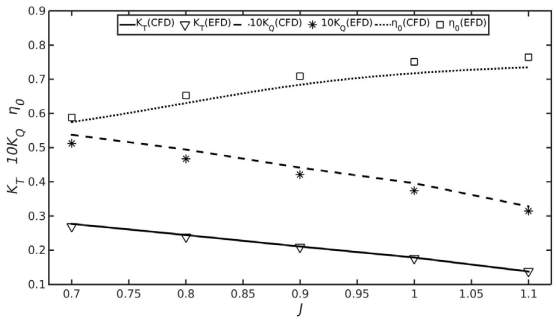

Fig. 12 Open-water performance curves of CRPs

Table 2 shows that predicted forces of single propeller are larger than front propeller when J is 1. Since the suction effect of the rear propeller on the front propeller, effective inflow velocity has increased to a certain extent. On the other hand, the efficiency of CRPs is 2.2% higher than single propeller. It is worth mentioning that, besides the distance of propellers' discs, the ratios of blade number and rotating speed also have large effect on efficiency of CRPs.

Table 2. Comparison between single propeller and CRPs

Items	K_T	$10K_Q$	Efficiency
Single propeller	0.229	0.473	0.694
Front propeller	0.190	0.412	0.661
Rear propeller	0.227	0.431	0.754
CRPs	0.417	0.843	0.709

Vortical Structure

Fig. 13 shows obvious differences of vortical structure between CRPs and single propeller. The vortical structure is colored by Ux/U_0 where U_0 is inflow velocity. As we can see, the velocity in x direction has greatly been improved by the rear propeller.

Pressure Distribution

Fig. 14 shows high pressure is mainly distributed around 0.7r where r is radius of propeller. Leading edge on pressure side encounters peak value of positive pressure. Peak value in single propeller is higher than front propeller'. Fig. 15 shows peak value of negative pressure is distributed around leading edge of suction side. Peak value of single propeller is 720pa higher than front propeller', therefore single propeller is easier to cause cavitating.

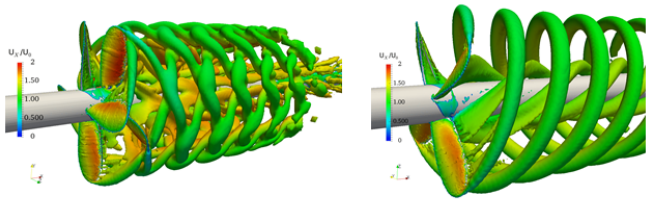

(a) CRPs (b) Single propeller

Fig. 13 Vortical structure at J=0.9

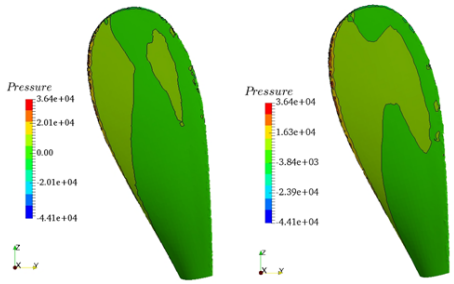

(a) CRPs (b) Single propeller

Fig. 14 Pressure distribution on pressure side

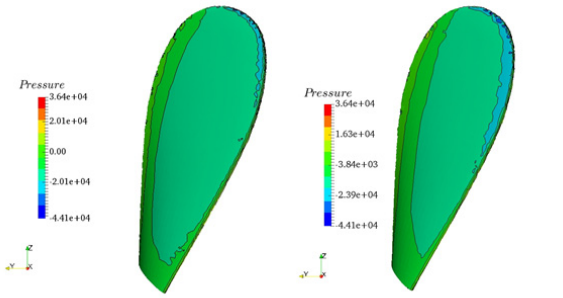

(a) CRPs (b) Single propeller

Fig. 15 Pressure distribution on suction side

Velocity Distribution

Fig. 16~17 are the velocity components distribution at different axial location. Ux, Ur and Ut are velocities in axial direction, radial direction and tangential direction respectively. Ur is defined to be positive outward, Ut is positive anticlockwise. Fig. 16 suggests how Ux is accelerated. Fig. 16 (a) says Ux will be accelerated drastically on the suction side of blade surface induced by the circulation effect of hydrofoil. After acceleration by rear propeller, the maximal magnitude of Ux is distributed around 0.7r. There are more interesting phenomena in Fig. 17. Fig. 17 (a) suggests that the higher Ur is centered in blade tips where there is a relative small area of negative velocity on the pressure side and a larger area of positive velocity on the suction side, Violent change of velocity will induce a strong tip vortex. Fig. 17 (c) suggests that the rear propeller will induce opposite Ur compared with the front propeller, so magnitude of Ur in wake field of CRPs has been greatly reduced. Fig. 18 shows that there are small areas of velocity variation around the blade tips which will induce strong tip vortex. Fig. 19 shows that, compared with single propeller, CRPs' magnitude of Ut in the wake field has been reduced drastically, that's why CRPs could achieve higher efficiency than single propeller. Meanwhile the lower magnitude of tangential and radial velocity with higher axial velocity will improve hydrodynamic performance of rudder.

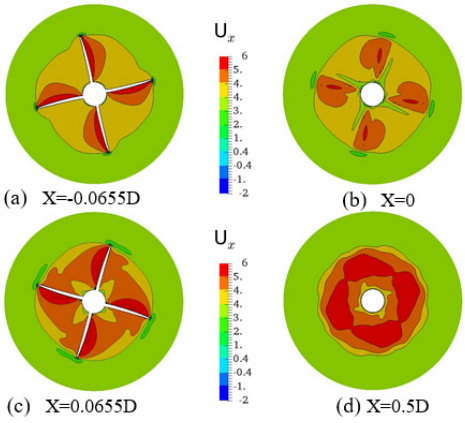

Fig. 16 Distribution of axial velocity at different axial location

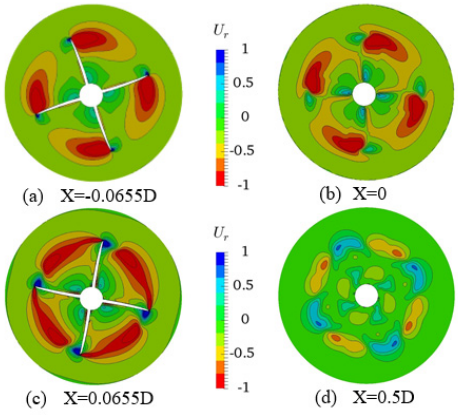

Fig. 17 Distribution of radial velocity at different axial location

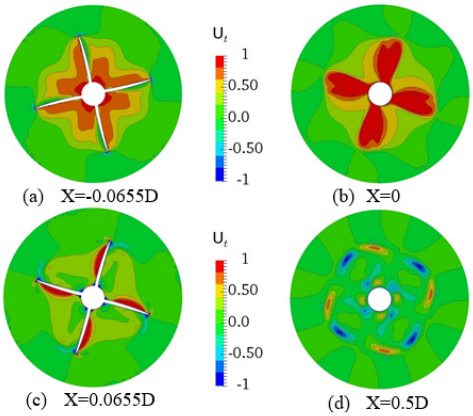

Fig. 18 Distribution of tangential velocity at different axial location

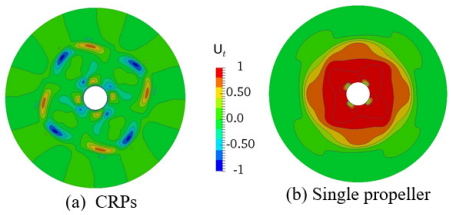

(a) CRPs (b) Single propeller

Fig. 19 Comparison of tangential velocity distribution

CONCLUSIONS

Based on sliding mesh method, the open-water performances of CRPs and single propeller have been investigated in detail. Time histories of K_T and K_Q exhibit obvious periodical unsteady feature with eight small periods after front or rear propeller rotates 360 degrees, Meanwhile, time-averages of K_T and K_Q agree well with their experimental counterparts, meaning that geometry models and numerical method used in this paper are reliable and credible. After comparison of calculated results of CRPs and single propeller, efficiency of CRPs is 2.2% higher than single propeller with the specific design parameters in this paper. What's more, vortical structure of CRPs is quite different from single propeller, rotational energy left by front propeller has been fully recovered by rear propeller as expected.

Future work will focus on the open-water performance of the so-called hybrid CRP podded propulsion system. The ratios of blade number, rotating speed and distance between front and rear propellers may greatly affect efficiency of such hybrid system. Therefore, it's necessary and meaningful to have a systematic investigation of those parameters' effect on the hybrid system.

ACKNOWLEDGEMENTS

This work is supported by the National Natural Science Foundation of China (51379125, 51490675, 11432009, 51579145), Chang Jiang Scholars Program (T2014099), Shanghai Excellent Academic Leaders Program (17XD1402300), Shanghai Key Laboratory of Marine Engineering (K2015-11), Program for Professor of Special Appointment (Eastern Scholar) at Shanghai Institutions of Higher Learning (2013022), Innovative Special Project of Numerical Tank of Ministry of Industry and Information Technology of China(2016-23/09) and Lloyd's Register Foundation for doctoral student, to which the authors are most grateful.

REFERENCES

Kim, S, Choi S (2002). "Model tests on propulsion systems for ultra large container vessel," *Proc 12th Int Offshore and Polar Eng Conf,* Kitakyushu, ISOPE, (4) 520-524.

Menter, F, Kuntz M, and Langtry R (2003). "Ten years of industrial experience with the SST turbulence model," *Turbulence, Heat and Mass Transfer*, (4) 625-632.

Miller, M (1976). "Experimental determination of unsteady forces on contra-rotating propellers in uniform flow," Technical Report No. AD-A032337, David W Taylor Naval Ship R&D Center.

Noack, RW, Boger, DA, Kunz, RF, and Carrica, PM (2009). "Suggar++: An improved general overset grid assembly capability," *Proc 47th AIAA Aerosp Sci Exhib*, 22-25.

Shen, Z, Wan, DC and Carrica, PM (2015). "Dynamic overset grids in OpenFOAM with application to KCS self-propulsion and maneuvering," *Ocean Eng*, 108, 287-306.

Wang G, Dong S (2007). "Theory and application of propeller for ship," Harbin Eng Univ Press.

Wang Z, Xiong Y and Qi W (2012)." Numerical prediction of open-water performance of contra-rotating propellers," *J Huazhong Univ of Sci & Tech*, 40(11), 77-88.

Wu J, Yin C, and Wan, D (2016). "Numerical prediction of open-water performance of propeller based on three methods," *Chin J Hydrodyn*, 31(2), 177-187.

Yang C, Tamashima M and Wang G (1991). "Prediction of the steady performance of contra-rotating propellers by lifting surface theory," *Transactions of the West-Japan Society of Naval Architects*, 82, 17-31.

Yang C, Tamashima M and Wang G (1992). "Prediction of the unsteady performance of contra-rotating propellers by lifting surface theory," *Transactions of the West-Japan Society of Naval Architects*, 83, 47-65.

Zhou H, Wan DC (2014). "Numerical simulation of the unsteady flow around wind turbines with different blades numbers," *J Hydrodyn Ser A*, 29(4): 444-453.